



Green Synthesis of ZnO Nanoparticles Using *Syzygium aromaticum* (Clove) Extract and Its Radio-Modifying Effect in Ehrlich Tumor-Bearing Mice

Hend A. Abd El Halim¹, Mohammed Salama², Ebtsam R. Zaher¹, Thanaa I. Shalaby³, Fawziya A.R. Ibrahim⁴, Hazem El Mansy⁵, Ahmed M. ElDrieny⁶, Adel A.-H. Abdel-Rahman⁷, Mohammed N. Salem⁸, Mohammed Abo El Ezz⁸, Shaymaa E. El Feky^{*1},

^aRadiation Sciences Department, Medical Research Institute, University of Alexandria, Alexandria, Egypt.

^bHistochemistry and Cell Biology Department, Medical Research Institute, Alexandria University, Alexandria, Egypt.

^cMedical Biophysics Department, Medical Research Institute, University of Alexandria, Alexandria, Egypt.

^dApplied Medical Chemistry Department, Medical Research Institute, Alexandria University, Alexandria, Egypt.

^eCancer Management and Research Department, Medical Research Institute, Alexandria University, Alexandria, Egypt.

^fRadiology and Medical Imaging Department, Faculty of Applied Health Sciences Technology, Pharos University, Alexandria, Egypt.

^gChemistry Department, Faculty of Science, Menaufia University, Shebin Elkom, Egypt.

^hM.Sc. of Radiobiology, Radiation Sciences Department, Medical Research Institute, University of Alexandria, Alexandria, Egypt



CrossMark

Abstract

Radioresistance is a major obstacle that hinders cancer treatment. Identification of agents that can modify malignant cells' response to radiation is a promising strategy to overcome this problem. We herein aimed to evaluate the potential radio-modifying effect of greenly synthesized zinc oxide nanoparticles (ZnO NPs) in sensitizing Ehrlich tumor-bearing mice to ionizing radiation (IR). *Syzygium aromaticum* (Clove) extract was used as a reducing agent for the green and sustainable synthesis of ZnO NPs. Characterization of ZnO NPs was done using transmission electron microscopy (TEM), ultraviolet-visible spectroscopy (UV-Vis), Fourier transform infrared spectroscopy (FT-IR), X-ray diffraction (XRD) and zeta potential measurement. Ehrlich-bearing mice were treated with 6 Gy IR either alone or in combination with 5 mg/100 g body weight ZnO NPs. Treatment response was assessed by monitoring tumor size, evaluation of apoptosis and oxidative stress markers, in addition to histopathological examinations. Our results indicated that the average size of synthesized ZnO NPs was 13.35±3.36 nm and XRD confirmed the hexagonal ZnO wurtzite structure. UV-Vis spectra revealed a strong absorption peak at 348 nm which is characteristic of ZnO. Treatment with a sublethal dose of ZnO NPs resulted in a significant reduction in tumor size accompanied by a significant increase in BAX/BCL2 gene expression ratio, upregulation of TXNIP relative gene expression, and decreased total antioxidant capacity in tumor tissues of mice treated with ZnO NPs prior to irradiation compared to those of mice treated with radiation alone with almost no detectable hepatic or renal toxicity. This significant influence of ZnO NPs on sensitizing tumors to IR through induction of apoptosis and increasing oxidative stress in tumor cells suggests that ZnO NPs can be a promising biocompatible agent for future applications.

Keywords: Zinc Oxide; Nanoparticles; Green Synthesis; Clove; Radiosensitizers; Apoptosis; Oxidative Stress

1. Introduction

The burden of cancer incidence and mortality is rapidly growing worldwide, despite all the great efforts employed for its prevention and curation. Of all types of cancer, breast cancer is the most diagnosed and the leading cause of death among females [1]. There are various treatment modalities available including radiotherapy, where about 70% of breast cancer patients benefit from radiotherapy either with curative or palliative intent [2]. However, cancer cells may acquire radioresistance by adaptation to the radiation-induced alterations through activation of some transcription factors. Those cells alongside with the inherently radioresistant cells, escape the lethal effects of radiation and repopulate leading to recurrence and treatment failure [3]. Hence, it is critical to question the efficacy of the current treatment modalities and how to improve it.

*Corresponding author e-mail: shaymaa.elfeky@alexu.edu.eg ; (Shaymaa E. El Feky).

Received Date: 15 November 2024, Revised Date: 27 December 2024, Accepted Date: 30 December 2024

DOI: 10.21608/EJCHEM.2024.334797.10810

©2025 National Information and Documentation Center (NIDOC)

The ultimate solution to overcome cancer cell radiation resistance is using radiosensitizers. Radiosensitizers are administered prior to radiotherapy to increase tumor cell death while exempting normal cells [4]. However, developing an ideal radiosensitizer is extremely challenging and new candidates should be experimented. The development of nanoparticles (NPs) based radiosensitizers received great attention, due to their exquisite physicochemical properties including biocompatibility, intrinsic radiosensitive activities, high loading abilities of multiple types of drugs, and the enhanced permeability and retention effects in tumor tissue [5]. Also, they have enormous applications in various fields including pharmaceuticals, diagnostic imaging, chemotherapy, and drug delivery over the past years [6].

The use of metal NPs is emerging, with zinc oxide (ZnO) NPs being commonly used in biomedical applications due to the unique physical and chemical characteristics of ZnO in addition to their low cost and non-toxicity. Akhtar *et al.*, reported that ZnO NPs selectively trigger the formation of reactive oxygen species and induce apoptosis in cancer cells [7]. Several studies revealed its role in drug-delivery and its antimicrobial, anticancer, antioxidant, and anti-inflammatory effects [8].

There are various methods for ZnO NPs synthesis; however, the use of plants, plant parts or microorganisms as a greener eco-friendly method is preferable to maintain a safe environment. The green synthesis beside being clean and non-toxic is also cost-effective and reproducible [9]. Clove oil (*Syzygium aromaticum* L.) is an essential oil that is rich in reducing agents. It contains about 90% of eugenol-organic phenol with reductive properties. Moreover, most of the ingredients of essential oils are lipophilic and can envelop the metal NP's surface and stabilize them [10]. Herein, we aimed to evaluate the radiosensitizing effect of greenly synthesized ZnO NPs in Ehrlich tumor-bearing mice.

2. Results

Physicochemical Characterization of Greenly Synthesized ZnO NPs

A precipitate of ZnO was formed following the addition of clove extract to zinc nitrate hexahydrate precursor demonstrating the phytosynthesis of ZnO NPs. The calculated yield of synthesis reaction was 87.5% which supports the use of plant-mediated synthesis for production of ZnO NPs with an efficiency that is comparable to chemical production.

The characterization data of greenly synthesized ZnO NPs prepared in the current study are illustrated in Fig. 1. The size and morphology of ZnO NPs were pictured by transmission electron microscope (TEM) pictures at a magnification of 100 nm which shows that ZnO NPs' size ranged from 9.94 - 19.65 nm with a mean value of 13.35 ± 3.36 nm (Fig. 1a).

Fig. 1b displays the ZnO NPs' X-ray diffraction (XRD) analysis pattern. The hexagonal ZnO wurtzite structure is well-indexed to all of the diffraction peaks (JCPDS no. 36-1451). The high purity of the synthesized products was confirmed by the absence of diffraction peaks associated with the impurity in the XRD pattern. The diffractogram showed three intense diffraction peaks with 2θ values of 31.68° , 34.34° , and 36.17° , which are attributed to (100), (002), and (101) crystallographic reflection planes. Moreover, other strong diffraction peaks were also observed, showing 2θ values of 47.45° , 56.53° , 62.81° , 67.92° , and 69.03° , respectively were indexed to (102), (110), (103), (112) and (201) planes, without other phases detected that indicate to purity of the NPs prepared (Fig. 1b).

As shown in Fig. 1c, for ZnO NPs synthesized with clove extract, the characteristic peak absorbance value was found at around 348 nm, according to the ultraviolet-visible spectroscopy (UV-Vis) absorption spectrum. The spectrum showed no other peaks, indicating that pure ZnO NPs had successfully formed.

The Fourier-transform infrared (FT-IR) spectra indicate various characteristic bands for various functional groups on greenly synthesized ZnO NPs. We observed that the bands are at 3450 cm^{-1} , 2273 cm^{-1} , 2071 cm^{-1} , 1635 cm^{-1} , 1384 cm^{-1} , 1075 cm^{-1} , and 572 cm^{-1} . The band formed at 572 cm^{-1} is indicated to ZnO stretching vibration. Aromatics compounds were formed and indicated by C=C-C, a symmetric stretch of -C-C=C and C=C was observed at around 1635 cm^{-1} , 1384 cm^{-1} , and 1075 cm^{-1} . The alcoholic group -COH shows due to the bending vibration, and the secondary amine NH_2 shows due to stretching vibration and the band formed at 1635 cm^{-1} shows due to -C=O groups from the conjugation in the aromatic ring. The strong band at 1384 cm^{-1} was observed due to the glycosidic linkage of C-O-C and secondary alcoholic groups (Fig. 1d).

The stability of ZnO NPs synthesized using clove extract was quantified by the measurements of zeta potential. The NPs are sufficiently stabilized in solutions when their zeta potential is $> 20\text{ mV}$ or $< -20\text{ mV}$. The zeta potential value of ZnO NPs synthesized using clove extract was found to be -16 mV indicating negative surface charges on the NPs.

ZnO NPs Modified Radiation Effect on Tumor Size in Ehrlich Tumor-Bearing Mice

We herein experimented the radio-modifying effect of ZnO NPs in experimental mice bearing Ehrlich solid tumors. We monitored mice weight and tumor size before and after the treatment. Our data indicate that there was a slight decrease in mice weight after treatment with no significant difference between ZnO NPs treated and untreated groups (Fig. 2a). Regarding the tumor volume, the control group showed a significant increase in the tumor volume when comparing tumor size at the start and end of treatment ($p < 0.001$); however, groups treated with either ZnO or IR showed insignificant changes in tumor volume ($p = 0.615$ and 0.124 , respectively). Nevertheless, mice treated with ZnO+IR showed a significant decrease in tumor size 6 days after treatment compared with their size before treatment ($p < 0.001$). We further calculated the percentage of change in tumor size for all experimental groups which indicated that the tumor volume was significantly lower in all treated groups compared to the control ($p < 0.05$), also ZnO+IR showed a significant further reduction in tumor volume compared to ZnO or IR alone (Fig. 2b).

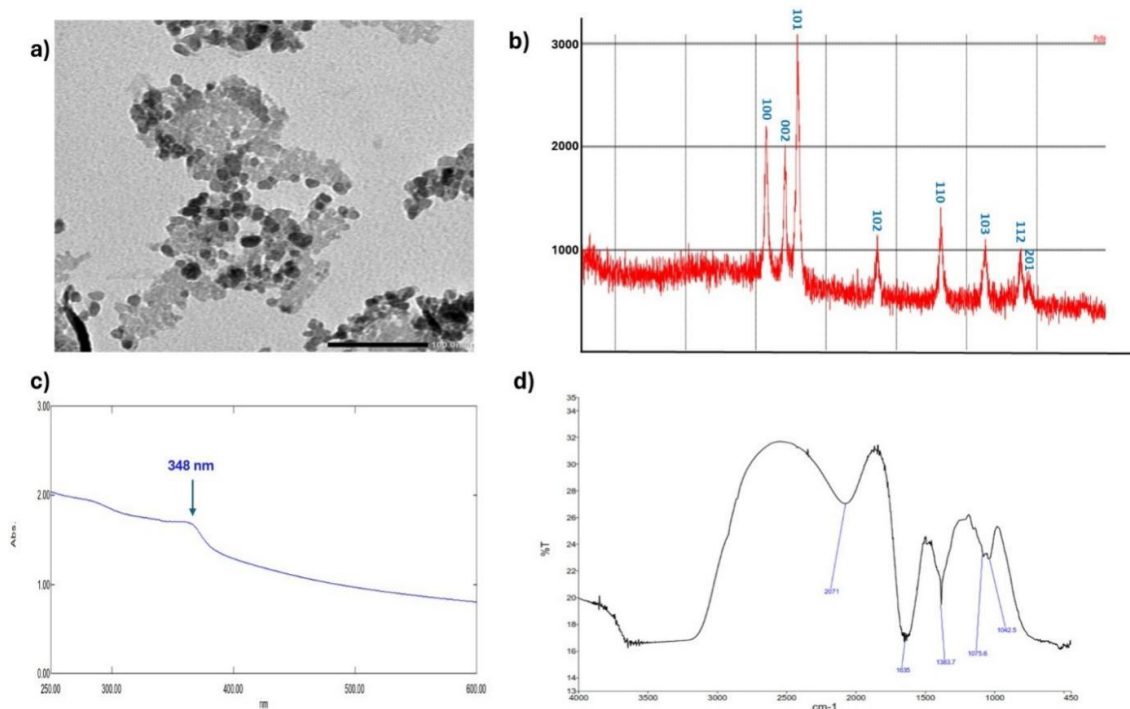


Fig.1. Characterization of Greenly Synthesized ZnO NPs. a) TEM picture displaying size and morphology of ZnO NPs, b) XRD spectrum of ZnO NPs with diffraction range of 20-80°, c) UV-Vis spectral analysis of ZnO NPs in wavelength range of 200-600 nm, and d) FT-IR patterns of ZnO NPs in the wavenumber range of 4000–500 cm^{-1} .

Investigation of Hepatic and Renal Functions in Response to IR and ZnO Treatment Combinations

Investigation of serum liver functions of Ehrlich-bearing mice showed that ZnO NPs treatment did not exert a hepatotoxic effect represented in the insignificant change in aspartate transferase (AST) levels and yet a significant reduction in alanine transferase (ALT) levels in ZnO NPs treated mice compared to the control group ($p < 0.001$). Although treatment with IR leads to a significant increase in serum ALT levels, ZnO+IR treated group showed a significant decrease in both ALT and AST levels compared to mice treated with IR alone ($p < 0.001$) indicating a positive effect of ZnO NPs in mitigating the radiation-induced hepatotoxicity in mice (Fig. 3a&b). Our data also showed that serum kidney functions were not negatively affected by ZnO NPs treatment. ZnO alone lead to a significant decrease in urea levels compared to untreated mice ($p < 0.001$); however, urea levels in both IR and ZnO+IR groups were insignificantly different from control group (Fig 3c). Creatinine levels did not show any significant change in all treated groups compared to control group ($p = 0.172$) (Fig. 3d).

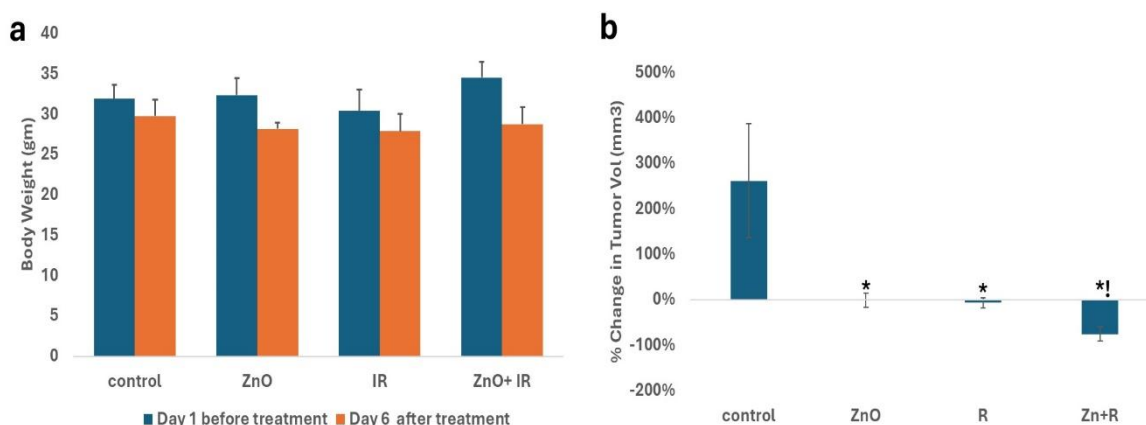


Fig. 2. a) Ehrlich tumor-bearing mice weight and b) Percentage of change in Ehrlich tumor volume (mm^3) before and 6 days after ZnO NPs and IR treatment, $n=8$, $p < 0.05$.

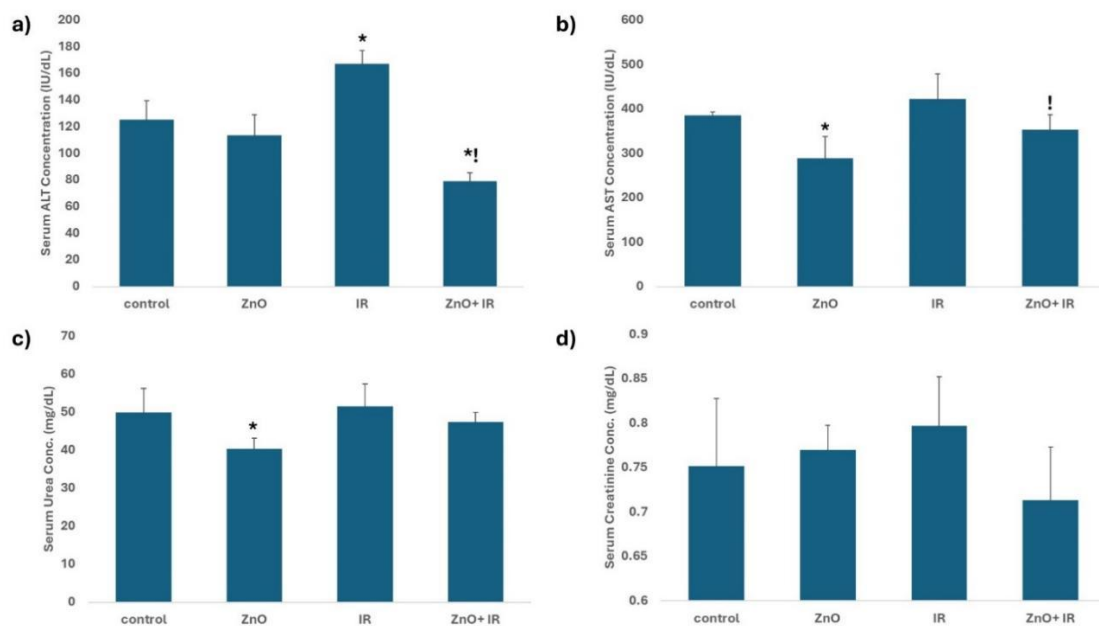


Fig. 3. Graphical presentation of liver functions [a) ALT & b) AST] and kidney functions [c) Urea & d) Creatinine] in sera of Ehrlich tumor-bearing mice, where * represents significant difference compared to control group, and ! represents significant difference from IR group, $n=8$, $p<0.05$.

ZnO NPs Enhances Radiation-Induced Apoptosis in Tumor Tissue

On the molecular level, we assessed the relative gene expression of the anti-apoptotic BCL2 and its competitor pro-apoptotic BAX in the tumor tissue. BCL2 expression showed a significant upregulation in groups treated with either ZnO NPs or IR alone compared to control group ($p<0.001$), while it showed an insignificant downregulation in ZnO+IR group (Fig. 4a). BAX, however, was significantly upregulated in all treated groups compared to untreated control ($p<0.001$) (Fig. 4b). We then calculated the BAX/BCL2 ratio which indicated susceptibility of tumor cells to undergo apoptosis. BAX/BCL2 ratio peaked in ZnO+IR treated group with a value of 3.65 ± 0.50 compared to 1.04 ± 0.27 for control, and 2.12 ± 0.47 for IR group ($p<0.001$) indicating a significant enhancement of radiation-induced apoptosis due to ZnO NPs combination (Fig. 4c).

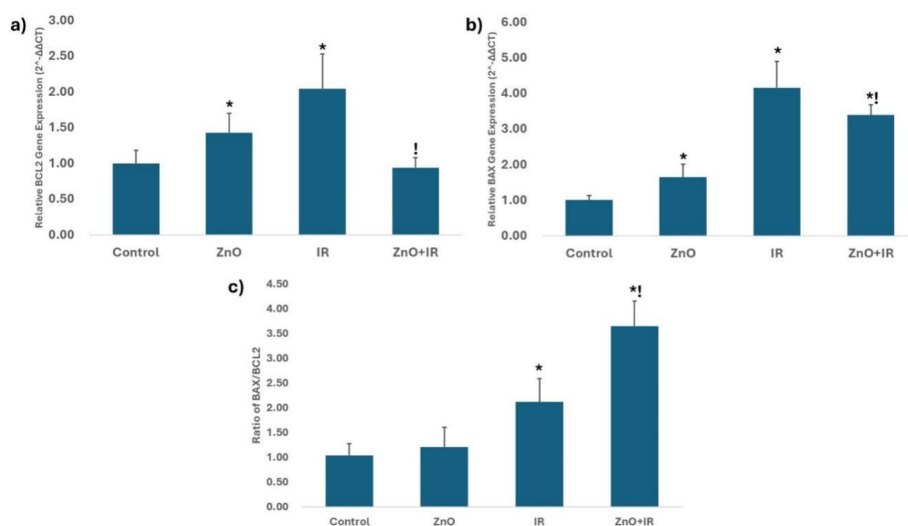


Fig. 4. Graphical Presentation of Relative Gene Expression of Apoptotic Markers a) BCL2 and b) BAX and c) BAX/BCL2 calculated ration in tumor tissue, where * represents significant difference from control group, and ! represents difference from IR treated group, $n=8$, $p<0.05$.

ZnO NPs Modulated Radiation-Induced Oxidative Stress in Tumor Tissue

As a marker of oxidative stress, we evaluated the relative gene expression of TXNIP in tumor tissue (Fig. 5a). TXNIP expression significantly upregulated in groups that were treated with IR, and in combination with ZnO NPs when compared to untreated group ($p < 0.001$). The total antioxidant capacity (TAC) of tumor tissues showed a significant decrease in tumor tissues treated with IR alone compared to control group. Treatment with ZnO NPs lead to a further reduction in TAC when injected either alone ($p = 0.007$), or in combination with IR ($p < 0.001$) when compared to untreated mice (Fig. 5b).

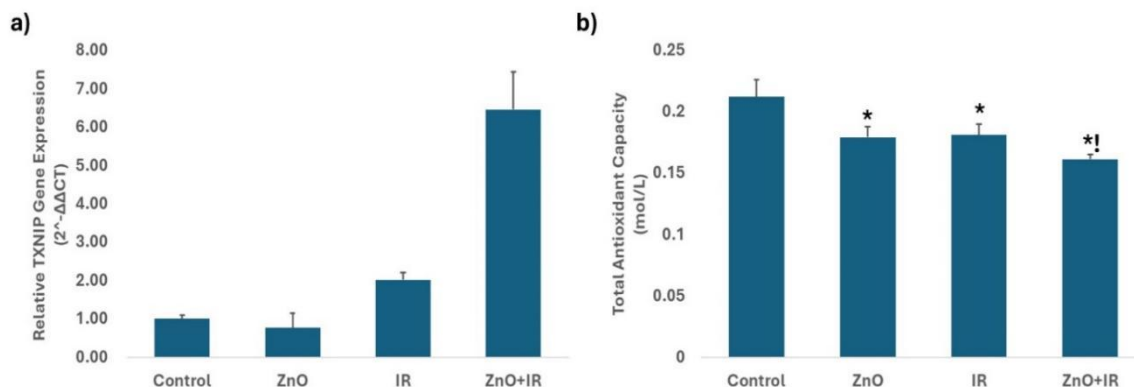


Fig. 5. Graphical Presentation of a) Relative gene expression of TXNIP and b) Quantitative determination of TAC in tumor tissue, where * represents significant difference from control group, and ! represents difference from IR treated group, $n = 8$, $p < 0.05$.

Histopathological Examination of Tumor, Liver and Kidney Tissues

The examination of untreated Ehrlich tumor sections stained with hematoxylin and eosin (H&E) showed a well-defined capsule composed of neoplastic cells infiltrating the skeletal muscles (Fig. 6a). The examination of the Ehrlich tumor sections of the group treated with ZnO NPs showed mild necrosis in the focal areas of the tumor surrounded by granulation tissue with reported decrease in the vascularization (Fig. 6b). For mice treated with IR alone, tumor sections showed moderate necrosis in the area of tumor appeared as homogenous structureless material, of note, the muscle fibers still invaded by the tumor cells (Fig. 6c). Tumor sections from ZnO+IR group showed a significant regression of tumor with observed wide area of necrosis (Fig. 6d).

Regarding the effect of treatment on liver tissues, histopathological analysis of sections obtained from untreated group showed classical hepatic lobules with normal liver architecture. The plates of hepatocytes as seen radiated outwards from a central vein. Hepatocytes showed abundant granular, eosinophilic cytoplasm with observed centrally placed round nuclei (Fig. 6e). Also, liver sections obtained from ZnO treated group showed normal hepatic architecture (Fig. 6f). Histopathological analysis of liver sections obtained from irradiated mice showed dissociation of hepatic cords with observed dilatation of hepatic sinusoids and cytoplasmic vacuolation. Of note, aggregation of infiltrating inflammatory cells was reported (Fig. 6g), while those of mice treated with ZnO+IR showed histoarchitecture near normal with less cytoplasmic vacuolation (Fig. 6h). Histopathological examination of kidney tissue was also conducted to evaluate the possible toxicity of treatment plan. Untreated mice kidneys showed normal renal cortex with its glomeruli, proximal convoluted tubules, distal convoluted tubules, and macula densa (Fig. 6i). Also, ZnO treated group showed normal renal architecture with normal renal glomeruli (Fig. 6j). For mice treated with IR alone, kidney sections showed dilatation and congestion of renal blood vessels with degenerative changes observed in renal tubules. Of note, some glomeruli showed atrophy (Fig. 6k), while in those treated with ZnO+IR, kidney sections showed restoration of normal kidney structure. Of note, no atrophied glomeruli were observed (Fig. 6l).

3. Discussion

NPs have the potential to improve the stability and solubility of encapsulated cargos, promote transport across membranes and prolong circulation times to increase safety and efficacy. Thus, NPs research has been widespread, generating promising results in vitro and in small animal models [14]. Metal and metal oxide NPs have shown wide applications in numerous fields. ZnO NPs are among the most widely used NPs, and have been implicated in number of sectors owing to their distinct physical and chemical properties. ZnO is bio-safe and biocompatible with distinctive abilities [15].

Green synthesis of NPs makes use of environmentally-friendly, non-toxic and safe reagents. This study introduces a green synthesis method to produce ZnO NPs using hydrodistilled extracts from clove (*Syzygium aromaticum*) flower buds.

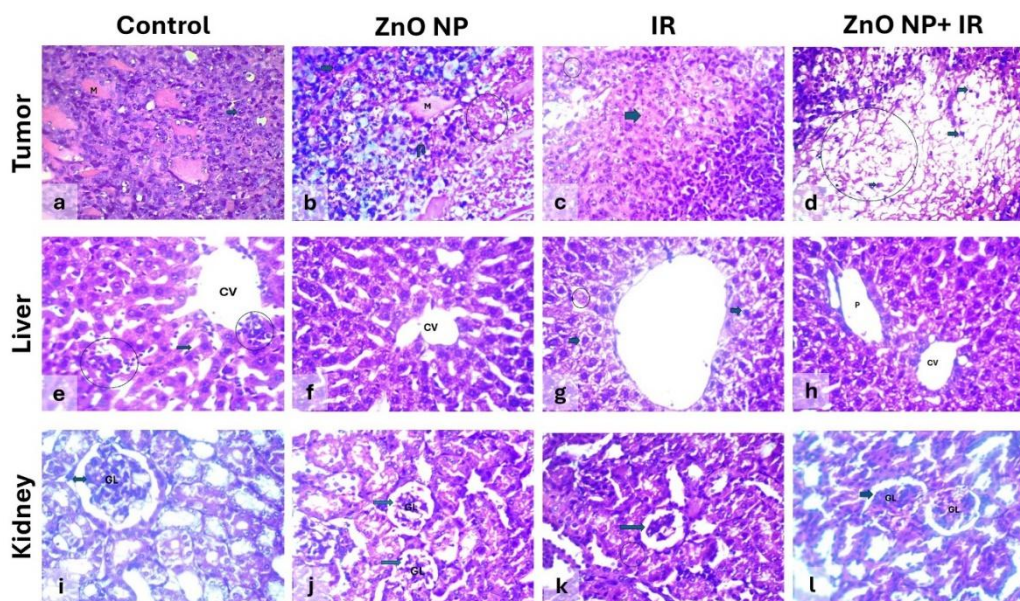


Fig. 6. Histopathological Photomicrographs for Solid Ehrlich Carcinoma tumors of a) untreated mice showed giant tumor cells (arrow) invading skeletal muscle fibers (M), **b)** ZnO NPs group showed mild necrosis in the focal areas of the tumor (circle) with observed cytoplasmic vacuolation and pyknotic nuclei in tumor cells (curved arrow), **c)** IR group showed moderate area of necrosis (arrow) with observed pyknosis (circle), and **d)** ZnO+IR group showed wide area of necrosis with dramatic regression of tumor (circle) with observed increase in the apoptotic cells (arrow). **Liver sections of e)** untreated mice showed normal hepatic architecture with dilated central vein and observed inflammatory cells infiltration (circle), **f)** ZnO NPs group showed classic hepatic lobule **g)** IR group showed histopathological changes with observed cytoplasmic vacuolation (arrow) and necrosis (circle), and **h)** ZnO+IR group showed normal hepatic portal area (P) and central vein (CV) with less cytoplasmic vacuolation. **Kidney sections of i)** untreated group showed normal histological structure with intact bowman capsule space (arrow) and glomerulus (GL), **j)** ZnO NPs group showed normal GL, **k)** IR group showed histopathological change of the tissue with observed atrophy of GL (arrow) and spread of necrotic area (circle), and **l)** ZnO+IR showed GL with normal size and normal bowman capsules space (arrow) (H&E stain, $\times 400$)

Clove is a member of the Myrtaceae family that is rich in bioactive compounds including eugenol [16] which have been reported to have anti-inflammatory, antibacterial, antifungal, and antioxidant activities [17-18]. The hydrodistillation method offers significant benefits by preserving volatile compounds that are sensitive to heat and oxidation. This method produces high-purity extracts with few impurities, and improved environmental sustainability by guaranteeing high-quality extracts with intact aromatic and bioactive substances. Furthermore, this process eliminates the need for intensive heat processing, and makes it easier to form ZnO NPs with little alkali. Therefore, the phenolic compounds in clove extract serve as organic stabilizing agents to help ZnO NPs form [19]. Characterization results of the prepared ZnO NPs in the current study are consistent with the previously reported morphological and optical characteristics of ZnO. The existence of an absorbance peak at 348 nm aligns with prior reports that ZnO NPs display optical absorption between 340 and 380 nm [20, 21]. Additionally, the prepared NPs' observed zeta potential value in this study is comparable to what has been found in other pertinent studies. It shows the green synthesized ZnO NPs' relative stability and dispersity, which is explained by the functional groups from clove extract that are present on their surfaces, and act to cap and stabilize the NPs [22, 23].

Radiosensitizers reduce cancer cell tolerance to IR and facilitates/augments cancer cell damage. Nanomaterials have the ability for localizing energy deposition under irradiation. This approach increases radiation absorption by cancer tissues, expanding the therapeutic window and, thus, increasing specificity and efficacy of treatment by IR [24]. In the current study, Ehrlich tumor-bearing mice have been used as an animal model to explore the radiosensitizing potential of ZnO NPs. The impact of single high dose (6 Gy) of radiation was monitored alone and in combination with ZnO NPs. The animals treated by ZnO NPs with radiation showed a much better response to radiation treatment than animal treated by radiation alone. Each of radiation and ZnO NPs presented an effective tumor volume control, but only their combination caused a significant reduction (possibly eradication) in tumor volume. Histopathological examination of the tumor tissues reflects the damaging impact of both IR and ZnO NPs on tumor cells but more importantly, it highlights the synergistic effect between IR and ZnO NPs in reducing tumor volume. These data showed that ZnO NPs exhibited *in vivo* anticancer effect against solid Ehrlich tumor-

bearing mice. This is in agreement with several publications reporting that combined treatment of NPs, specifically ZnO NPs, and IR significantly reduced tumor volume in mice bearing tumors [25-27]. This reduction in tumor volume is mostly due to enhanced apoptosis as indicated by the significant increase in BAX/BCL2 ratio. The apoptotic cascade is most probably derived by increased oxidative stress, as indicated by greatly increased TXNIP expression in tumor tissues and the significantly lowered TAC.

In the current study, the mice bearing solid Ehrlich tumors showed normal liver and kidney functions after exposure to radiation and/or treatment by ZnO NPs, as indicated by un-affected AST, ALT, urea, and creatinine levels. This might indicate that ZnO NPs are well tolerated at the dose used in the current study setting. Histopathological analysis of liver and kidney tissues of mice revealed a damaging effect of both IR and ZnO NPs; however, upon their combined administration, ZnO NPs displayed a protective effect for liver and kidney tissue against radiation damage. Quite contradictory results are noted regarding the impact of ZnO NPs treatment on animals. While some authors assume they exert a protective effect on vital organs [28-29], several publications reported their deleterious effects on animal vital organs, including kidneys and liver [30-32]. These contradictions, however, may be attributed, at least in part, to different production methods and conditions of ZnO NPs synthesis, with which size, shape, stability, and active capping groups of the resulting NPs differs. The monitoring of mice body weight (BW) also revealed a slight insignificant reduction after ZnO NPs treatment.

4. Experimental

Preparation of *Syzygium aromaticum* (Clove) Buds' Extract

Dry *Syzygium aromaticum* clove buds were purchased from the local market and the essential oils was extracted by using maceration method [11]. The buds were grinded into powder by using a clean electric miller, then 30 g were added to 150 ml of a 70:30 (V/V) mixture of distilled water and ethanol (Sigma-Aldrich, US, CAS #: 64-17-5). The mixture was then kept in dark for 24 h at 30°C followed by filtering through twofold layered muslin fabric and the supernatant was recovered by centrifugation at 4000 rpm for 10 min. The supernatant was sieved through Whatman no. 1 filter paper. A rotary evaporator (Steroglass, Italy) was then used to evaporate the ethanol at temperature of 60°C, rotation speed of 200 rpm and atmospheric pressure of 0.4 atm. The obtained solution was considered as mother extract and kept aseptically in a darker screw capped bottle at 4°C for further use.

Biosynthesis of ZnO NPs

Zinc nitrate ($Zn(NO_3)_2 \cdot 6H_2O$) (Sigma-Aldrich, US, cas # 10196-18-6), as the substrate, was mixed with the clove extract at a ratio of 1:5 (w/v). The solution was placed into an autoclave at a temperature of 121°C and a pressure of 1.5 atm for 15 min, and then transferred to a China dish and placed in a 350°C furnace for 2 h [12]. The yield of the final product was calculated using the following equation: Yield (%) = (experimental weight of ZnO/theoretical weight of ZnO)*100.

Characterization of ZnO NPs

Transmission electron microscope (TEM, JEOL X100, Japan) was used to determine the size and shape of prepared ZnO NPs. The structural properties and crystalline nature of ZnO NPs was analyzed by X-ray diffractometer (Shimaduz, XRD-7000, Maxima, Japan), operated at a voltage of 30 KV, a current of 30 mA, with $CuK\alpha$ radiation and analyzed between 5 and 100° (2 θ). The optical properties of ZnO NPs was characterized using UV-Vis spectrometry (Shimadzu UV-1800, Japan), where the absorption measurements were carried out at room temperature over the range of 200–600 nm. Metal oxide NP surface plasmon resonance (SPR) electrons display characteristic peaks at distinctive wavelengths. Fourier-transform infrared (FT-IR) spectra for ZnO NPs were obtained on a Shimadzu FT-IR-8400S (Tokyo, Japan), where 4-8 mg of samples were ground with 200 mg of potassium bromide, and compressed using Shimadzu compressor (Japan), then the prepared pellets were fixed on the holder of FT-IR spectroscopy to be scanned over the wave number range of 4000 to 400 cm^{-1} . The surface charge properties of the green synthesized ZnO NPs were measured by Zetasizer (Malvern Zetasizer Ultra, UK) and zeta potential was determined using ZS XPLORER v.1.3.2 software.

Experimental Animals and Treatment Protocol

The in vivo study design and handling procedures were revised and approved by Medical Research Institute Animal Care and Use Committee, Alexandria University (AU-012-23/1/29-2-1) for following international regulations. Thirty-two Swiss albino male mice (20-30 g) were used for the assessment of radio-modifying effect of ZnO NPs in vivo. Balb/C female mice with Ehrlich carcinoma cell ascites were obtained from Egyptian National Cancer Institute, Cairo University, Egypt. The ascitic fluid was collected from abdominal cavity, centrifuged at 400x to collect the cells, washed twice by phosphate-buffered saline (PBS), counted using hemocytometer, and cells were resuspended in PBS. Subsequently, a single dose containing approximately 2×10^6 cells were injected subcutaneously for solid tumor induction. Mice were monitored for solid tumor development and treatment application started when the larger diameter of most of the tumors reach 7 mm and confirmed by

histopathological examination. The 32 mice were randomly divided into 4 equal groups: Group I: untreated control, Group II: ZnO NPs (5 mg/100 g BW, 1/10 LD₅₀), Group III: 6 Gy IR, and Group IV: ZnO+IR (5 mg/100 g BW, 1/10 LD₅₀+6 Gy). According to this plan, mice in matched groups received intraperitoneal injections of ZnO NPs every other day for a total period of 6 days. On day 6, mice received a single dose of 6 Gy of X ray using PRIMUSTM Linear Accelerator (Siemens® Medical Solutions, Germany) at 300 cGy/min [13].

Mice Weight, Tumor Volume, and Sampling

The mice weight (g) and tumor volume were monitored at the start and end of the application of treatment protocol. A vernier caliper was used to measure the length and width of the tumor, and the volume was calculated using the equation: $V = a \times b^2 \times 0.5$; where, V is the tumor volume (mm³), and a and b are the longer and shorter diameter (mm), respectively.

After completion of the treatment plan, mice were euthanized using decapitation under anesthesia (1% isoflurane) and blood samples were collected by cardiac puncture. Serum was collected by centrifugation of clotted whole blood samples at 4000 rpm for 10 mins at 4°C. Solid tumors, livers and kidneys were excised and subdivided into two portions. The first portion was stored along with the collected serum samples at -80°C till further use. The second portion was preserved in formalin (10%) before it was processed and embedded in paraffin blocks for subsequent histopathological examination using hematoxylin and eosin (H&E) staining.

Gene Expression Analysis

Tumor tissue was homogenized in PBS, centrifuged to remove cell debris, and the supernatant was used to assess the relative gene expression of BAX, BCL2, and TXNIP. Total RNA extraction was carried out using commercially available kit (Qiagen, RNeasy Mini Kit #74104), and the concentration of the extracted RNA was measured by nanodrop (Thermo Scientific ND2000, USA). Following extraction of RNA, cDNA was synthesized using commercially available kit (Thermo Fisher Scientific, USA) using Applied Biosystems GeneAmp PCR System 9700 N8050200 thermal cycler with the following conditions: 25°C for 10 min, 37°C for 120 min, 85°C for 5 min, and 4°C on hold. cDNA was then stored at -20°C until quantitative real time PCR (qRT-PCR) experiments. For qRT-PCR, the primer sequences used were BAX: forward, 5' TCAGGATGCGTCCACCAAGAAG 3' and reverse, 5' TGTGTCCACGGCGGCAATCATC 3'; BCL2: forward, 5' ATCGCCCTGTGGATGACTGAGT 3' and reverse, 5' GCCAGGAGAAATCAAACAGAGGC 3'; TXNIP: forward, 5' CAGCAGTGCAAACAGACTTCGG 3' and reverse 5' CTGAGGAAGCTCAAAGCCGAAC 3', and GAPDH: forward, 5' GTCTCCTCTGACTTCAACAGCG 3' and reverse, 5' ACCACCCTGTTGCTGTAGCCAA 3'. The qRT-PCR reaction was performed using Maxima SYBR Green qPCR Master Mix (2X) (Thermo Fisher Scientific, USA) with cycling conditions as follows: an initial activation step of 10 min at 95°C; 45 cycles of 15 sec at 95°C, 30 sec at 54°C, and 30 sec at 72°C. Gene expression was normalized to the expression of GAPDH and quantified using the comparative cycle threshold ($\Delta\Delta Ct$) method.

Total Antioxidant Capacity Assay

The total antioxidant capacity (TAC) of tumor tissues after treatment with the greenly synthesized ZnO NPs were assessed using a commercially available kit (Biodiagnostics, Egypt). The working reagent was prepared by mixing equal amounts of chromogen and enzyme buffer. H₂O₂ substrate was added to blank and samples (0.5 ml), mixed, and then incubated for 10 mins at 37°C. The working reagent was added, mixed well, incubated for 5 min, then the absorbance (ABS) was measured at 505 nm (Stat Fax 2100 Microplate ELISA Reader, Awareness Technologies, USA). The TAC was calculated using the equation: $TAC (mmol/L) = (ABS_{blank} - ABS_{sample}) \times 3.33$.

Biochemical Markers

Kidney functions including urea and creatinine, and liver functions including alanine transferase (ALT) and aspartate transferase (AST) were assessed in mice sera using commercially available kits (Spectrum Diagnostics, Egypt) according to manufacturers' instructions.

Statistical Analysis

Statistical analysis was performed with statistical program IBM SPSS Statistics for windows, where appropriate statistical tests were used for results comparisons and analysis. Data are presented as the mean \pm standard deviation (SD). $P \leq 0.05$ was considered to indicate a statistically significant difference. The statistical analysis was done using one-way ANOVA to compare between more than two groups, and post hoc test (Tukey) for pairwise comparisons

5. Conclusions

In conclusion, ZnO NPs at sub-lethal dose may be considered a good radiosensitizer, which augmented the damaging effect of ionizing radiation. It works through inducing excessive apoptosis by increasing oxidative stress in cells. When administered in

vivo concomitantly with radiation, it significantly enhanced the effect of radiation with almost no detectable toxicity to the kidneys or to the liver.

6. Conflicts of Interest

There are no conflicts to declare.

7. Formatting of Funding Sources

The authors declare that no funds, grants, or other support were received during the preparation of this manuscript.

8. References and Bibliography

- [1] Bray F, Laversanne M, Sung H, Ferlay J, Siegel RL, Soerjomataram I, Jemal A. Global cancer statistics 2022: GLOBOCAN estimates of incidence and mortality worldwide for 36 cancers in 185 countries. *CA Cancer J Clin.* 2024;74(3):229-263. doi: 10.3322/caac.21834.
- [2] Maliko N, Stam MR, Boersma LJ, Vrancken Peeters MTFD, Wouters MWJM, KleinJan E, Mulder M, Essers M, Hurkmans CW, Bijker N. Transparency in quality of radiotherapy for breast cancer in the Netherlands: a national registration of radiotherapy-parameters. *Radiat Oncol.* 2022;17(1):73. doi: 10.1186/s13014-022-02043-0.
- [3] Galeaz C, Totis C, Bisio A. Radiation Resistance: A Matter of Transcription Factors. *Front Oncol.* 2021;11:662840. doi: 10.3389/fonc.2021.662840.
- [4] Gong L, Zhang Y, Liu C, Zhang M, Han S. Application of Radiosensitizers in Cancer Radiotherapy. *Int J Nanomedicine.* 2021 Feb 12;16:1083-1102. doi: 10.2147/IJN.S290438.
- [5] Song X, Sun Z, Li L, Zhou L, Yuan S. Application of nanomedicine in radiotherapy sensitization. *Front Oncol.* 2023;13:1088878. doi: 10.3389/fonc.2023.1088878.
- [6] Sim S, Wong NK. Nanotechnology and its use in imaging and drug delivery (Review). *Biomed Rep.* 2021;14(5):42. doi: 10.3892/br.2021.1418.
- [7] Akhtar MJ, Ahamed M, Kumar S, Khan MM, Ahmad J, Alrokayan SA. Zinc oxide nanoparticles selectively induce apoptosis in human cancer cells through reactive oxygen species. *Int J Nanomedicine.* 2012;7:845-57. doi: 10.2147/IJN.S29129.
- [8] Anjum S, Hashim M, Malik SA, Khan M, Lorenzo JM, Abbasi BH, Hano C. Recent Advances in Zinc Oxide Nanoparticles (ZnO NPs) for Cancer Diagnosis, Target Drug Delivery, and Treatment. *Cancers (Basel).* 2021;13(18):4570. doi: 10.3390/cancers13184570.
- [9] Perumal P, Sathakkathulla NA, Kumaran K, Ravikumar R, Selvaraj JJ, Nagendran V, Gurusamy M, Shaik N, Gnanavadeivel Prabhakaran S, Suruli Palanichamy V, Ganesan V, Thiraviam PP, Gunalan S, Rathinasamy S. Green synthesis of zinc oxide nanoparticles using aqueous extract of shilajit and their anticancer activity against HeLa cells. *Sci Rep.* 2024;14(1):2204. doi: 10.1038/s41598-024-52217-x.
- [10] Fizer MM, Mariychuk RT, Fizer OI. Gold nanoparticles green synthesis with clove oil: spectroscopic and theoretical study. *Appl Nanosci* 2022;12(3): 611–620 doi: 10.1007/s13204-021-01726-6
- [11] Abubakar AR, Haque M. Preparation of Medicinal Plants: Basic Extraction and Fractionation Procedures for Experimental Purposes. *J Pharm Bioallied Sci.* 2020;12(1):1-10. doi: 10.4103/jpbs.JPBS_175_19.
- [12] Safawo, T, Sandeep BV, Pola S, Tadesse A. Synthesis and characterization of zinc oxide nanoparticles using tuber extract of anchote (*Coccinia abyssinica* (Lam.) Cong.) for antimicrobial and antioxidant activity assessment. *Open Nano* 2018;3,25. doi: 10.1016/j.onano.2018.08.001.
- [13] Nakhla S, Albeherly B, Shawky S, Lotfi S, Kotb M, El-Bassiouni E, El-Abd E. Pre-irradiation effects of ectoine on radiation-induced cardiotoxicity in female Swiss albino mice model. *Arch Pharm Sci Ain Shams Univ* 2022;6(2),169-180. doi: 10.21608/aps.2022.148701.1094
- [14] Mitchell MJ, Billingsley MM, Haley RM, Wechsler ME, Peppas NA, Langer R. Engineering precision nanoparticles for drug delivery. *Nat Rev Drug Discov.* 2021;20(2):101-124. doi: 10.1038/s41573-020-0090-8.
- [15] Mandal AK, Katuwal S, Tettey F, Gupta A, Bhattarai S, Jaisi S, Bhandari DP, Shah AK, Bhattarai N, Parajuli N. Current Research on Zinc Oxide Nanoparticles: Synthesis, Characterization, and Biomedical Applications. *Nanomaterials (Basel).* 2022;12(17):3066. doi: 10.3390/nano12173066.
- [16] Razafimamonjison G, Michel J, Thierry D, Panja R, Fania F, Pascal D. Bud, leaf and stem essential oil composition of *Syzygium aromaticum* from Madagascar, Indonesia and Zanzibar. *Int J Basic Appl Sci.* 2014;3,224.
- [17] Otunola GA. Culinary Spices in Food and Medicine: An Overview of *Syzygium aromaticum* (L.) Merr. and L. M. Perry [Myrtaceae]. *Front Pharmacol.* 2022;12:793200. doi: 10.3389/fphar.2021.793200.

- [18] da Silva FFM, Monte FJQ, de Lemos TLG, do Nascimento PGG, de Medeiros Costa AK, de Paiva LMM. Eugenol derivatives: synthesis, characterization, and evaluation of antibacterial and antioxidant activities. *Chem Cent J*. 2018;12(1):34. doi: 10.1186/s13065-018-0407-4.
- [19] Haiouani K, Hegazy S, Alsaedi H, Bechelany M, Barhoum A. Green Synthesis of Hexagonal-like ZnO Nanoparticles Modified with Phytochemicals of Clove (*Syzygium aromaticum*) and *Thymus capitatus* Extracts: Enhanced Antibacterial, Antifungal, and Antioxidant Activities. *Materials (Basel)*. 2024;17(17):4340. doi: 10.3390/ma17174340.
- [20] El Golli A, Contreras S, Dridi C. Bio-synthesized ZnO nanoparticles and sunlight-driven photocatalysis for environmentally-friendly and sustainable route of synthetic petroleum refinery wastewater treatment. *Sci Rep*. 2023;13(1):20809. doi: 10.1038/s41598-023-47554-2.
- [21] Mongy Y, Shalaby T. Green synthesis of zinc oxide nanoparticles using *Rhus coriaria* extract and their anticancer activity against triple-negative breast cancer cells. *Sci Rep*. 2024;14(1):13470. doi: 10.1038/s41598-024-63258-7.
- [22] Fernandes CA, Jesudoss M N, Nizam A, Krishna SBN, Lakshmaiah VV. Biogenic Synthesis of Zinc Oxide Nanoparticles Mediated by the Extract of *Terminalia catappa* Fruit Pericarp and Its Multifaceted Applications. *ACS Omega*. 2023;8(42):39315-39328. doi: 10.1021/acsomega.3c04857.
- [23] Iqbal J, Abbasi BA, Yaseen T, Zahra SA, Shahbaz A, Shah SA, Uddin S, Ma X, Raouf B, Kanwal S, Amin W, Mahmood T, El-Serehy HA, Ahmad P. Green synthesis of zinc oxide nanoparticles using *Elaeagnus angustifolia* L. leaf extracts and their multiple in vitro biological applications. *Sci Rep*. 2021;11(1):20988. doi: 10.1038/s41598-021-99839-z.
- [24] Generalov R, Kuan WB, Chen W, Kristensen S, Juzenas P. Radiosensitizing effect of zinc oxide and silica nanocomposites on cancer cells. *Colloids Surf B Biointerfaces*. 2015;129:79-86. doi: 10.1016/j.colsurfb.2015.03.026.
- [25] Khafaga DSR, Eid MM, Mohamed MH, Abdelmaksoud MDE, Afify M, El-Khawaga AM, Abdelhakim HK. Enhanced anticancer activity of silver doped zinc oxide magnetic nanocarrier loaded with sorafenib for hepatocellular carcinoma treatment. *Sci Rep*. 2024;14(1):15538. doi: 10.1038/s41598-024-65235-6.
- [26] Sayed HM, Said MM, Morcos NYS, El Gawish MA, Ismail AFM. Antitumor and Radiosensitizing Effects of Zinc Oxide-Caffeic Acid Nanoparticles against Solid Ehrlich Carcinoma in Female Mice. *Integr Cancer Ther*. 2021;20:15347354211021920. doi: 10.1177/15347354211021920.
- [27] Huang C, Chen T, Zhu D, Huang Q. Enhanced Tumor Targeting and Radiotherapy by Quercetin Loaded Biomimetic Nanoparticles. *Front Chem*. 2020;8:225. doi: 10.3389/fchem.2020.00225.
- [28] Rahman HS, Othman HH, Abdullah R, Edin HYAS, Al-Haj NA. Beneficial and toxicological aspects of zinc oxide nanoparticles in animals. *Vet Med Sci*. 2022;8(4):1769-1779. doi: 10.1002/vms3.814.
- [29] Abdel-Magied N, Ahmed AG, Abo Zid N. Possible ameliorative effect of aqueous extract of date (*Phoenix dactylifera*) pits in rats exposed to gamma radiation. *Int J Radiat Biol*. 2018;94(9):815-824. doi: 10.1080/09553002.2018.1492165.
- [30] Xiao L, Liu C, Chen X, Yang Z. Zinc oxide nanoparticles induce renal toxicity through reactive oxygen species. *Food Chem Toxicol*. 2016;90:76-83. doi: 10.1016/j.fct.2016.02.002.
- [31] Al-Zahaby SA, Farag MR, Alagawany M, Taha HSA, Varoni MV, Crescenzo G, Mawed SA. Zinc Oxide Nanoparticles (ZnO-NPs) Induce Cytotoxicity in the Zebrafish Olfactory Organs via Activating Oxidative Stress and Apoptosis at the Ultrastructure and Genetic Levels. *Animals (Basel)*. 2023;13(18):2867. doi: 10.3390/ani13182867.
- [32] Abouzeinab NS, Kahil N, Fakhruddin N, Awad R, Khalil MI. Intraperitoneal hepato-renal toxicity of zinc oxide and nickel oxide nanoparticles in male rats: biochemical, hematological and histopathological studies. *EXCLI J*. 2023;22:619-644. doi: 10.17179/excli2023-6237.